A Study of the Mechanism of the Reaction between Ozone and the Chlorine Atom Using Density Functional Theory

James Tyrrell* and Tapas Kar†

Department of Chemistry and Biochemistry, Southern Illinois University, Carbondale, Carbondale, Illinois 62901

Libero J. Bartolotti

North Carolina Supercomputing Center, 3021 Cornwallis Rd., Research Triangle Park, North Carolina 27709

Received: May 22, 2000; In Final Form: February 22, 2001

Density functional calculations of the potential energy surface for the reactions $^2Cl + {}^1O_3 \rightarrow {}^2ClO + {}^3O_2$ and $^2ClO + {}^3O \rightarrow {}^2Cl + {}^3O_2$ have been carried out using the Perdew−Wang functionals for exchange and for correlation with a variety of basis sets. For the former reaction, a number of stationary points have been identified corresponding to both a trans and a cis pathway. Both pathways have an early transition state, followed by a weakly bound complex, and are connected through a late transition state leading to the products. All stationary points on the surface lie at energies lower than those of the initial reactants. The early transition state and complex are planar in both paths, whereas the late, common transition state is nonplanar. The early transition state is not a transition state for the reaction path but connects two alternative but equivalent ways in which the complex distorts out of the plane. The region between the late transition state and the products is complicated by a mixing of O_2 spin states. The latter reaction has a much simpler reaction surface, involving an early transition state with a very low barrier leading directly to the products with high exothermicity. These DFT results for the former reaction fail to identify an early transition state found by previous investigators (14) using QCISD and CASSCF methods, raising questions about the applicability of DFT methods for transition state calculations. There are, however, some areas of agreement between this and the prior study. However, neither study satisfactorily replicates the experimentally determined classical barrier for the reaction or unambiguously determines whether an intermediate complex ClO−O_2 is present.

Introduction

The importance of chlorine as a catalyst in the destruction of ozone in the stratosphere has been recognized for some time.[1] A simplified form of the mechanism by which a radical species such as the chlorine atom can catalytically break down ozone can be represented as follows:[2]

$$^2X + {}^1O_3 \rightarrow {}^2XO + {}^3O_2$$

$$^2XO + {}^3O \rightarrow {}^2X + {}^3O_2$$

where X = Cl, OH, or NO.

Particular attention has been paid to the chlorine-catalyzed reaction because of the concern that the chlorine atoms are generated by the photolytic cleavage of chlorofluorocarbons (CFCs) released into the atmosphere.[2(a)] Numerous studies of the kinetics of the reaction between various radical species and ozone have been carried out, and Table 1 summarizes the results of some of these studies.[3] As can be seen, there is relatively little variation in the pre-exponential factors, and the rate constants appear to correlate with the electron affinity of the radical species rather than with the exothermicity of the reaction.[4] This led to the suggestion that the structure of the transition state for these reactions was insensitive to the nature of the radical species X and that the reaction would likely proceed through an early transition state.[4] It was further suggested that the correlation with radical species electron affinities would indicate that, in these reactions, a transfer of electron density from the HOMO orbital of ozone to the singly occupied radical molecular orbital would occur.[4]

TABLE 1: Empirical Rate Data for the Reactions:[a,b] $^2X + {}^1O_3 \rightarrow {}^2XO + {}^3O_2$ and $^2XO + {}^3O \rightarrow {}^2X + {}^3O_2$

	$^2X + {}^1O_3 \rightarrow {}^2XO + {}^3O_2$			$^2XO + {}^3O \rightarrow {}^2X + {}^3O_2$		
^2X	A	E_a	k_{220}	A	E_a	k_{220}
H	1.4×10^{-10}	3.9	1.7×10^{-11}	2.3×10^{-11}	∼0	2.3×10^{-11}
OH	1.6×10^{-12}	7.8	2.2×10^{-14}	3.5×10^{-11}	∼0	3.5×10^{-11}
NO	3.8×10^{-12}	13.1	2.9×10^{-15}	9.3×10^{-12}	∼0	9.3×10^{-12}
Cl	2.8×10^{-11}	2.1	8.7×10^{-12}	7.7×10^{-11}	1.1	4.3×10^{-11}

[a] Ref 3. [b] A and k_{220} are in units of cm^3 $molec^{-1}$ s^{-1} and E_a is in units of kJ mol^{-1}.

The asymmetric species ClO−O_2 has been suggested as a reaction intermediate,[5] but a matrix isolation study of the Cl + O_3 reaction revealed no trace of infrared absorptions for such a species[6] though ClO bands were identified. This result would suggest the likelihood that if ClO−O_2 is a reaction intermediate, it should be very short-lived. This conclusion would also tend to be supported by ab initio calculations carried out on the ClO_3 species by Rathmann and Schindler[7] and by Radom et al.[8] Rathmann and Schindler[7] showed that the association of O_2 and

* Corresponding author. E-mail: tyrrell@chem.siu.edu.
† Present address: Department of Chemistry, Utah State University, Logan, Utah.

10.1021/jp001868e CCC: $20.00
Published on Web 03/28/2001

ClO to form ClO—O_2 was endothermic by 13 kcal/mol. Radom et al.[8] found that the ClO_3 structure found by Rathmann and Schindler[7] did not persist when higher-level calculations were carried out, and they concluded that there was no stable ClO_3 complex but did not rule out the possibility of a van der Waals type of complex.

Several photolytic studies of the Cl + O_3 reaction have shown that the ClO product is formed with considerable vibrational excitation,[9,10] suggesting that the dominant exothermic process corresponded to the formation of the Cl—O bond. On the other hand, while electronically excited states of O_2 ($^1\Delta_g$ or $^1\Sigma_g^+$) are possible, no experimental evidence for the production of such species has been observed.[11]

A many-body expansion method was used by Farantos and Murrell[12] to determine an analytical function for the potential surface of ^{2}A ClO_3. They found an early transition state corresponding to attack by the Cl along the axis of one of the O—O bonds of ozone. The barrier height was found to be 0.34 kcal/mol, consistent with the experimentally determined value of 0.5 kcal/mol. Classical trajectory calculations using this surface led to an estimate of the room-temperature rate constant as 1.34×10^{-11} cm^3 molecule^{-1} s^{-1}, in good agreement with the experimental value. These calculations also showed no indication of a long-lived complex on the reaction path and that the ClO product was primarily forward-scattered with respect to the Cl in the center of mass (CM) system with significant vibrational and rotational energy. The O_2 product, on the other hand, showed little vibrational excitation.

The most recent studies of the Cl + O_3 reaction are a crossed molecular beam study by Zhang and Lee[13] and an ab initio study by Hwang and Mebel.[14] In the molecular beam study, a range of CM collision energies from 6 to 32 kcal/mol were used. A significant fraction of the total available energy is channeled into product translation, with the ClO being sideways- and forward-scattered with respect to the Cl atom. The authors conclude that the reaction occurs through a coplanar direct reaction mechanism, with attack by the chlorine on a terminal oxygen of the ozone. There is no evidence for a long-lived complex intermediate. The coplanar path best explains the wide range of CM angles into which the ClO product is scattered and the sideways scattering of the ClO at low collision energy. The authors do indicate that their results do not exclude the possibility of an out-of-plane channel. While channels involving O_2 ($^1\Delta_g$) and O_2 ($^1\Sigma_g^+$) are spin-allowed and energetically possible, no evidence for such channels was found.

The ab initio study by Hwang and Mebel[14] uses a variety of methods ranging from MP2 to CASPT2 and MRCI, though most of their data are obtained at the MP2 level and/or use MP2 optimized geometries to do single-point calculations at the higher levels of theory. The differences between the results to be reported here and those of Hwang and Mebel[14] are substantial, but there are some areas of agreement. These authors observe an early transition state which is nonplanar. They also observe a barrier between the reactants and this nonplanar transition state of anywhere from 37 kcal/mol at the lowest level of theory (MP2) to 4.6 kcal/mol at the QCISD(T) level. It is not surprising that their MP2 results are not reliable, considering the fact that this method has been shown to be inappropriate for the treatment of ozone (15—22 and Table 2) and would presumably be suspect for a transition state which is still very reactant-like. What is interesting is that their QCISD optimization of this first transition state (TS1) agrees so well with the result of their MP2 calculation in both geometry and frequencies but is substantially different in its estimation of the classical barrier. However, as they point out, their classical barrier is still at least 1 order of magnitude greater than experimentally determined barriers for this reaction (Table 1).

TABLE 2: Equilibrium Geometry (distance r_e in Å and Angle θ in deg) and Harmonic Vibrational Frequencies (ν in cm^{-1}) of the $^1A_1$ State of Ozone

method	ref	r_e	θ	ν_1(a1)	ν_2(a1)	ν_3(b2)
CISD/DZP	15	1.271	116.2	1234	745	1352
CASSCF/DZP	16	1.296	116.5	1098	689	989
CCSD/DZP	17	1.263	117.4	1256	748	1240
B—CCD/DZP	18	1.260	117.3	1264	756	1302
CCSD(T)/DZP	19	1.287	116.8	1129	703	976
B—CCD(T)/DZP	18	1.288	116.8	1127	703	1097
CCSDT/DZP	19	1.286	116.7	1141	705	1077
CISD[TQ]/DZP	18	1.281	116.7	1166	716	1138
B—P/DZP	21	1.290	118.0	1187	690	1087
MP2=Full/6-311G*	this work	1.283	116.9	1177	750	2288
pw91pw91/6-31+G*	this work	1.182	118.1	1187	699	1079
pw91pw91/aug-cc-pVQZ	this work	1.272	118.2	1187	714	1066
B3LYP/6-31+G*	this work	1.263	118.1	1258	733	1220
B3LYP/6-311+G*	this work	1.256	118.5	1246	747	1184
experiment	20	1.272	116.8	1135	716	1089

Hwang and Mebel's MP2 reaction surface begins with a nonplanar transition state and proceeds through a nonplanar complex in which the Cl—O bond is essentially formed (1.713 Å), but surprisingly, the O—O(Cl) bond is still very much present (1.436 Å), which would argue for a fairly stable complex. Hwang and Mebel point out that this complex is similar to the one calculated by Rathmann.[7] However, as previously pointed out, this structure did not persist when higher-level calculations were carried out.[8] Their reaction path then proceeds via a second nonplanar transition state (TS2), almost identical in geometry to the complex, to a planar complex with very little change in geometry or energy. This second transition state (TS2) is a transition state between the nonplanar and planar forms of the complex. Higher-level calculations on these complexes (B and C in their notation) by Hwang and Mebel failed to affirm the existence of these complexes. Their final step involves a planar transition state (TS3), which is actually lower in energy than the planar complex (G2(MP2)//MP2/6-311G(d)), and from there by an exothermic process (~16 kcal/mol) to the products. It is not clear why this final step should be so exothermic since the Cl—O bond and the O—O bond of the O_2 fragment are essentially fully formed in TS3 while the O—O(Cl) bond at 1.644 Å is still partially present. It is not clear from their published results whether any attempts were made to optimize the transition states TS2 and TS3 at a a higher level than MP2. A reasonable summary of their results would indicate a reaction path involving an early nonplanar transition state with a classical barrier, relative to the reactants, of 4—5 kcal/mol. This is followed by an exothermic process leading, possibly, to the formation of a weakly bound complex which either directly dissociates or dissociates through transition state TS3 with negligible classical barrier to the products.

The purpose of this study is to use density functional theory, which has been shown to be effective in representing multi configuration molecules such as ozone, to explore the stationary points on the reaction surface, first, of ozone and the chlorine radical and, second, of chlorine monoxide and the oxygen atom. Concern has been expressed about the adequacy of density functional calculations in systems whose intermolecular interactions are dominated by dispersion.[23] It is not clear, however, whether this means that the density functional method is inappropriate for all transition state calculations. It is also not clear at this time whether the problem lies with the exchange

correlation functional or with the use of a single-determinant (integer occupation numbers) solution.

Computational Section

All calculations were carried out using the density functional method and the Perdew−Wang[24] functionals for exchange and correlation (pw91pw91). This method was used in part because ozone is not well represented by a single electron configuration, i.e., [core...] $4b_2^2 6a_1^2 1a_2^2\ {}^1A_1$, but requires, at a minimum, the inclusion of a doubly excited configuration, i.e., [core...] $4b_2^2$-$6a_1^2 2b_1^2\ {}^1A_1$. As a consequence, the standard perturbative approach to including electron correlation (MP2), which assumes a single reference electron configuration, fails to accurately treat the structure and harmonic frequencies (refs 15−22 and Table 2). The RMP2 method not only gives a bond length (using a 6-31G* basis) that is too long by 0.027 Å but also leads to extreme error in determining the antisymmetric stretching frequency, ν_3 (2373 calcd vs 1089 expt).[21] While the UMP2 method improves on the harmonic frequencies, it still leads to an incorrect ordering of the ν_1 and ν_3 frequencies. Murray, Handy, and Amos[21] have shown that the density functional method performs well on molecules such as ozone in that it appears to be able to account for the multireference character of the wave function. These authors used the Kohn−Sham treatment with Becke exchange and Lee−Yang−Parr correlation functionals (B-LYP) as well as Perdew(1986) correlation functions (BP). The latter method gave somewhat better results. In the current work Perdew−Wang (91) functionals have been used for both exchange and correlation. This functional is an analytic fit to a generalized gradient approximation, and it satisfies various sum rules, scaling relations, and limiting forms for regions of high and low density. The basis sets used were 6-31+G*, 6-311+G*, aug-cc-pVDZ, cc-pVQZ, and aug-cc-pVQZ. All calculations were performed using Gaussian 98.[25]

Full geometry optimizations were run with all basis sets to locate the stationary points on the surface. The harmonic vibrational frequencies were also determined at the stationary points to identify minima and transition states and to obtain zero-point vibrational energy corrections. The intrinsic reaction coordinate method, IRC,[26] was used to follow minimum energy paths, where possible, from the transition states to the corresponding minima.

Results and Discussion

Each stationary point on the surface was optimized, and harmonic frequencies were determined using all of the basis sets. Since these results were consistent, the results discussed here will be those obtained using the aug-cc-pVQZ basis set, unless otherwise specified. Figure 1 shows all the stationary points on the surface and sketches out the reaction paths. Figure 2 and Table 3 summarize the structural and vibrational data for all of the stationary points on the trans and cis pathways. Figure 3 diagrams the energetics of the trans and cis pathways.

Intrinsic reaction coordinate (IRC) calculations were carried out along the forward and reverse minimum energy paths from each transition state to the closest minima. For transition state TS1 in both trans and cis pathways, the minimum-energy pathway begins by bending out of the plane in one of the two possible directions but always ends up at either the trans or the cis complex. In the case of the symmetric transition state in the cis pathway (cis-sym-TS), the IRC for this transition state led to the cis complex but with the chlorine bound to one or the other of the terminal oxygens. Finally, in the case of transition-state TS2, the IRC follows the reverse path to the cis complex

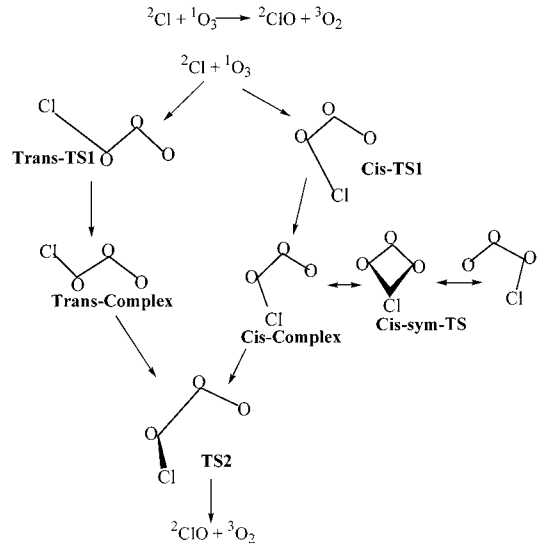

Figure 1. Stationary points and sketch of the trans (left) and cis (right) pathways of the $^2Cl + {}^1O_3 \rightarrow {}^2ClO + {}^3O_2$ reaction.

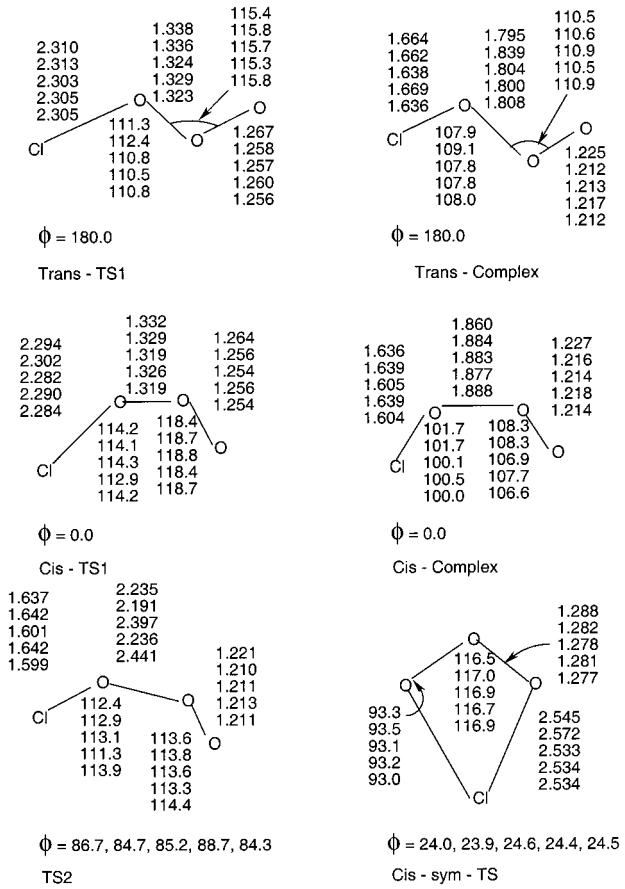

Figure 2. pw91pw91 geometric parameters of various stationary points along the trans and cis pathways of the $^2Cl + {}^1O_3 \rightarrow {}^2ClO + {}^3O_2$ reaction. The five values refer to 6-31+G*, 6-311+G*, cc-pVQZ, aug-cc-pVDZ, and aug-cc-pVQZ, respectively.

but is unable to proceed along the forward path by more than a few steps before encountering a minimum and halting.

We further investigated the energy surface around the first transition state (TS1) and found that there is no minima prior to this transition state along the reaction path. The chlorine atom approaches the terminal oxygen in either a trans or a cis manner along a barrierless path with an exothermicity (corresponding to the energy difference between the reactants and transition state TS1) of 8.81 or 10.83 kcal/mol (both ZPE corrected) for

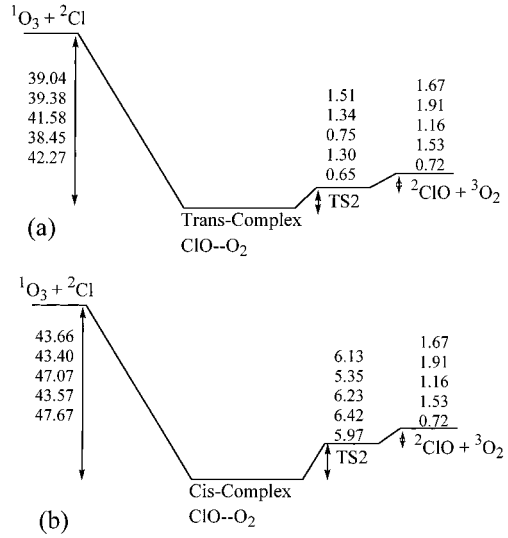

Figure 3. pw91pw91 potential energy surfaces [(a) trans and (b) cis pathways] of the $^2Cl + {}^1O_3 \rightarrow {}^2ClO + {}^3O_2$ reaction. The five values refer to 6-31+G*, 6-311+G*, cc-pVQZ, aug-cc-pVDZ, and aug-cc-pVQZ, respectively. Energy differences are ZPE corrected and in kcal/mol.

TABLE 3: Vibrational Frequencies (cm $^{-1}$) and Zero-Point Energies (ZPE in kcal/mol) of the Various Stationary Points in the $^2Cl + {}^1O_3 \rightarrow {}^2ClO + {}^3O_2$ Reaction Calculated Using the pw91pw91/aug-cc-pVQZ Method

systems	frequencies	ZPE
trans TS1	134*i*, 111, 211, 651, 818, 1181	4.25
trans complex	83, 157, 252, 558, 790, 1475	4.74
cis-sym-TS1	423*i*, 116, 257, 691, 838, 1185	4.42
cis complex	195, 263, 373, 548, 833, 1470	5.26
cis TS2	274*i*, 173, 300, 739, 956, 1103	4.68
TS2	40*i*, 54, 123, 150, 822, 1538	3.84

the trans or cis path, respectively. At this point on the reaction surface, the system becomes nonplanar as the chlorine singly occupied p orbital attempts to overlap with the π system of the ozone. The detailed energy surface at this point shows the dihedral angle changing by several degrees ($\sim$10°) with essentially no other change in the system, including its energy and spin distribution. At this point, the complex accesses a very exothermic path involving formation of the Cl−O bond and concurrent weakening of the O−O(Cl) bond, leading directly to the trans or cis ClO−O_2 complex. The transition state in this case really corresponds to a decision point as to the choice of equally acceptable ways of distorting out of the plane. While it is technically a transition state between two equivalent paths leading to the same reaction complex, it is not a true transition state for this reaction because there is no barrier associated with it along the reaction path. However it should be emphasized that in this region the energy is essentially constant while the system adopts a nonplanar structure before proceeding to the complex.

At this point, it is important to compare our results for this early transition state with those of Hwang and Mebel[14] because this is the only stationary point for which these authors provide an optimized geometry at other than the MP2 level. Again, it should be emphasized that the MP2 method has been shown to be inadequate in representing molecules requiring multiconfiguration wave functions, whereas density functional methods appear to handle such molecules rather well.[18,21,27] Specifically, they report optimized geometries for this transition state using the 6-311G* basis at the MP2, QCISD, and CASSCF[17,12] levels, all in close agreement as to the geometry and all indicating a dihedral angle of 85.6° (MP2), 82.5° (QCISD), or 82.4° (CASSCF). It should be pointed out that their geometry is very similar to that of our TS1 transition state, with the exception that ours is planar (trans and cis). While our TS1 transition state is not a true transition state for the reaction path, it does lie in a region of the potential energy surface where the system acquires a significant degree of nonplanarity with little or no change in energy before proceeding on to the complex. The QCISD and CASSCF calculations of Hwang and Mebel,[14] which should be superior to the DFT calculations, clearly demonstrate the existence of a transition state for the reaction in this region of the energy surface. The DFT calculations are more ambiguous but do indicate a flattening of the energy surface in this region, corresponding to a nonplanar distortion of the system and a negligible or nonexistent classical barrier.

TABLE 4: Total Atomic Spin Densities of the Stationary Points in the cis and trans Surface of the $^2Cl + {}^1O_3 \rightarrow {}^2ClO + {}^3O_2$ Reaction

atoms	reactant	cis/trans TS1	cis/trans complex	TS2	product
O		−0.096/−0.158	0.533/0.610	0.966	1.0
O		−0.028/−0.058	0.492/0.505	0.939	1.0
O		0.325/0.362	−0.021/−0.081	−0.629	0.675
Cl	1.0	0.799/0.854	−0.004/−0.034	−0.275	0.325

As already noted, a symmetric transition state (cis-sym-TS), not present in the trans path, was observed in the cis path. The IRC clearly indicates this is a transition state for the transformation from the cis planar complex where the chlorine is attached to one of the terminal oxygens to another totally equivalent cis planar complex in which the chlorine is attached to the other terminal oxygen of the ozone. As one would anticipate, the barrier to this transfer is rather high at 38.43 kcal/mol (ZPE corrected) and this transition state plays no part in the reaction under investigation.

The next stationary point along the reaction surface is the ClO−O_2 complex, which has been previously postulated as a reaction intermediate.[5] In this complex, the Cl−O bond is almost fully formed (1.636 Å in the trans complex and 1.604 Å in the cis complex), and the O−O(Cl) bond is very weak (1.808 Å in the trans complex and 1.888 Å in the cis complex). The step involving the formation of the Cl−O bond is highly exothermic (>30 kcal/mol, relative to the first "transition state") and would support the experimental evidence that the Cl−O product is vibrationally excited.[9,10] The length of the O−O(Cl) bond would imply a very weak, almost van der Waals like complex, which suggests a very short-lived complex, in agreement with the lack of any experimental observation of it[6] and the theoretical predictions based on studies of various ClO_3 species.[7,8] This appears to be further supported by the barrier found between the complex and the final, common transition state (TS2). In the case of the trans path, this barrier is only 0.65 kcal/mol (ZPE corrected) though it is significantly greater in the cis path (5.97 kcal/mol). It is interesting to note that in both the trans and cis complex, the unpaired electron is associated with the O_2 fragment of the complex (Table 4). The results of Hwang and Mebel[14] and the current work both suggest, at best, a very weakly bound complex.

The final stationary point on the surface is transition-state TS2. This transition state is nonplanar and is extremely product-like, having bond lengths for the Cl−O and O_2 fragments essentially identical to those of the product species as well as a spin distribution identical to that of the product species (Table 4). The IRC from this transition state connects in one direction with the cis complex but is unable to move more than a few points along the other direction. A plot of the optimized energies

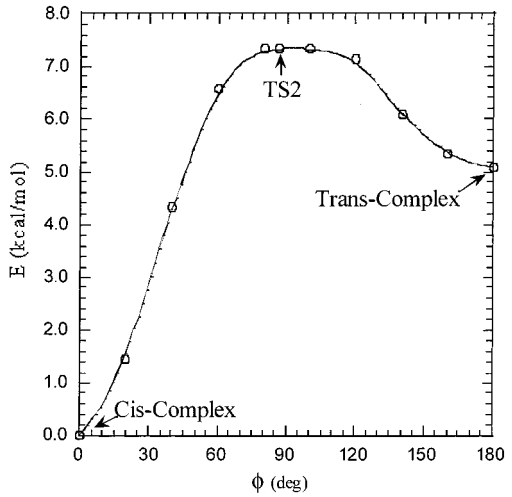

Figure 4. Potential energy curve and ClOOO dihedral angle (ϕ) of the $^2Cl + {}^1O_3$ reaction obtained by pw91pw91/6-31+G*.

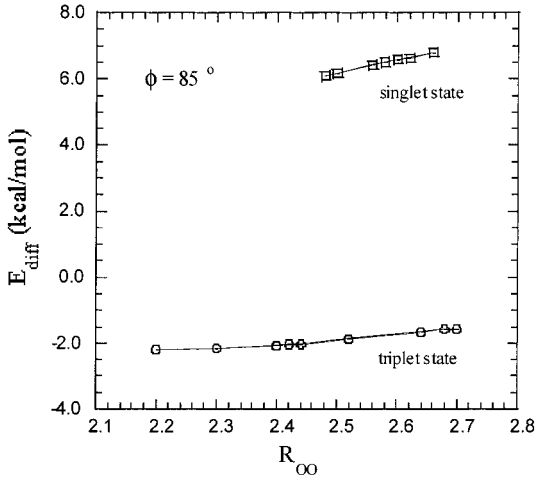

Figure 5. Variation of pw91pw91/6-31+G* energy of triplet and singlet states of O_2 in ClO_3 with OO distance. Energy values are ZPE-corrected and relative to the total energy of the products $^2ClO + {}^3O_2$.

as a function of dihedral angle in this region of the surface, Figure 4, shows a smooth downward energy transition from the transition state to the cis complex, as described by the IRC, but there is a very flat energy region between the transition state and the dip to the energy of the trans complex. It would appear this flattened area coincides with the further path to eventual separation of the Cl−O and O_2 fragments along the O−O(Cl) direction. It should be noted that the apparent classical barrier between the transition-state TS2 and the trans complex (0.65 kcal/mol) is almost 1 order of magnitude smaller than the barrier between transition-state TS2 and the cis complex (5.97 kcal/mol), suggesting that the trans path is the more likely one.

What was at first surprising was that transition-state TS2 was 0.72 kcal/mol lower in energy than the final products. However, a survey of the surface in the region corresponding to R(O−O) distances of 2.2−3.0 Å and dihedral angles from 75−95° indicated optimized structures with an unusual scattering of total energies. These could be systematized when it was noted that the spin distribution in one part of the set corresponded to a singlet O_2 fragment while the other part of the set had a spin distribution corresponding to a triplet O_2 fragment. Figure 5 illustrates this result at a dihedral angle of 85°, where the energies are relative to those of the final products. Clearly, the actual structure in this region must be represented by at least two spin configurations, corresponding to the triplet and singlet

TABLE 5: Equilibrium Geometry (distance R in Å and Angle θ in deg), Harmonic Vibrational Frequencies (ν In cm $^{-1}$), and Zero-Point Energy (ZPE in kcal/mol) of the Various Stationary Points in the $^2ClO + {}^3O \rightarrow {}^2Cl + {}^3O_2$ Reaction Calculated Using the pw91pw91/6-31+G* Method

parameters	2ClO	4ClOO complex	4ClOO-TS	$^3O_2$
R(ClO)	1.619	1.648	1.695	
R(OO)		1.953	1.774	1.228
θ ClOO		119.7	143.3	
ν	829	103	271*i*	1558
		381	256	
		747	559	
ZPE	1.19	1.76	1.17	2.23

O_2 weakly bound to the doublet ClO. Inclusion of even a small amount of the singlet O_2 spin configuration should raise the energy of ClO_3 species above that of the products, which were defined as $^2ClO + {}^3O_2$. Because of the difficulty with the mixture of spin states, it is not clear exactly how transition-state TS2 connects with the products. The results would suggest however that the classical barrier between the complex and products would lie in the range of 0−1 kcal/mol. Again, this is in general, if not in detailed, agreement with the conclusions of Hwang and Mebel.[14]

Overall then, the DFT reaction pathway is highly exothermic, with an initial step involving coplanar approach of the chlorine to the ozone, followed by a distortion out-of-plane (by as much as 29°) to allow the chlorine orbital to overlap with the ozone π orbital. This distortion initially occurs with little change in the remainder of the geometry or the energy but rapidly finds a strongly exothermic path, involving formation of the Cl−O bond and weakening of the O−O(Cl) bond and a reversion to a planar structure for the ClO−O_2 complex. The exothermicity of this step would suggest a vibrationally excited Cl−O fragment, which is what is observed experimentally. The complex is very weakly bound and proceeds via at most a small classical barrier to the final transition state. This transition state is common to both paths but energetically more accessible by the trans path. The bond lengths of the two fragments and the spin distributions are essentially identical to those of the product species. The part of the reaction surface between this transition state and the products is complicated by a mixing of triplet and singlet states of the O_2 fragment and prevents us from fully characterizing this portion of the reaction path. While spin contamination in this portion of the potential energy surface could be a problem, it should be pointed out that the density functional method suffers less from spin contamination than conventional methods.[28]

The following reaction in the catalytic cycle

$$^2ClO + {}^3O \rightarrow {}^2Cl + {}^3O_2$$

has also been investigated. Both the low-spin and high-spin paths have been investigated. An MP2=FULL study of ^{2}ClOO using 6-31G*, 6-311G*, and 6-31+G* basis sets produced a bent transition state with R(Cl−O) = 1.6396 Å, R(O−O) = 1.7952 Å, and ClOO = 110.479° (with the 6-31+G* basis set), but this has a barrier relative to the reactants of 8.731 kcal/mol (ZPE corrected), which is more than 1 order of magnitude greater than the experimentally determined value (Table 1). On repeating this calculation for a doublet ClOO transition state using both the CCSD and the density functional method (pw91pw91/6-31+G*), we obtained no transition state, the only result being ClO + O or Cl + O_2. However, the density functional method did identify a ^{4}ClOO transition state, and Table 5 lists the

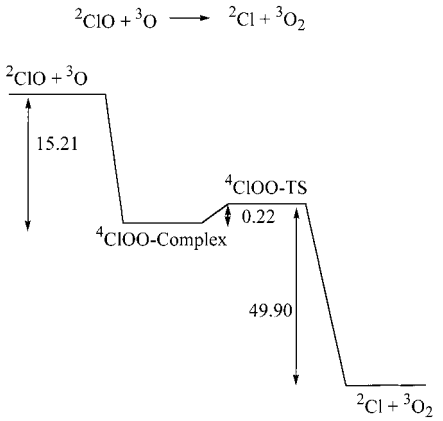

Figure 6. Potential energy diagram for the $^2ClO + {}^3O \rightarrow {}^2Cl + {}^3O_2$ reaction, calculated using pw91pw91/6-31+G* method. Energy differences are ZPE-corrected and in kcal/mol.

relevant parameters for the reactants, products, and the two stationary points. An IRC calculation from the transition state connects with a weak van der Waals like complex between the ClO and the O atom and with the product species for the reaction. The classical barrier to the reaction is 0.22 kcal/mol (ZPE corrected). Figure 6 provides an energy schematic for the reaction.

Conclusions

The structures, energies, and vibrational frequencies have been calculated for the reactants, products, and the stationary points on the reaction surfaces for the reaction of the chlorine atom with ozone and the reaction of chlorine monoxide with an oxygen atom. While a number of stationary points are found for the former reaction, they can be associated with either a trans or cis coplanar attack of the chlorine on the ozone. The apparent, early transition state observed in both the trans and cis paths is, in fact, a transition state between two equivalent paths associated with a nonplanar distortion of the system to allow for better overlap between the chlorine p orbital and the ozone π system. There is a flattening of the energy profile in this portion of the energy surface associated with a nonplanar distortion of the reaction system. Whereas Hwang and Mebel's results[14] clearly indicate a transition state for the reaction in this region with a classical barrier of 4−5 kcal/mol, the DFT results are more ambiguous, suggesting at best a flattening of the energy surface in this region. The symmetric transition state found only in the cis path is one between two equivalent cis complexes, with the chlorine attached to one or other of the terminal atoms. The late, nonplanar transition state is common to both paths, with a barrier in the trans path of around 0.5 kcal/mol, though because of mixing of spin states it is not possible to link it directly to the products. In the latter reaction, the stationary points are a weakly bound ClO−O complex, followed by an early transition state with a barrier of 0.22 kcal/mol.

Though the overall profile of the energy is quite different for the DFT and Hwang and Mebel[14] results, there are points of similarity. Hwang and Mebel clearly identify an early transition state, though the classical barrier is too high when compared to experimental results. The DFT calculations indicate a flattening of the energy surface in the same region as that of Hwang and Mebel's early transition state, indicating little or no classical barrier. Both results indicate at best a weakly bound complex, which then dissociates with little or no classical barrier to the products. The DFT method fails in clearly identifying an early transition state, but the QCISD and CASSCF methods, while pinpointing this early transition state, fail to adequately replicate the experimentally determined classical barrier. Clearly, there is still a need for further investigation of this reaction surface to resolve the discrepancies between the experimental and theoretical classical barriers and to affirm or deny the existence of any intermediate complex.

References and Notes

(1) Stolarski, R. S.; Cicerone, R. J.*Can. J. Chem.* **1974**, *52*, 1610.

(2) (a) Molina, M. J.; Rowland, F. S. *Nature* **1974**, *249*, 810. (b) Cicerone, R. J.; Stolarski, R. S.; Walters, S. *Science* **1974**, *185*, 1165. (c) Crutzen, P. J. *Geophys. Res. Lett.* **1974**, *1*, 205. (d) Wofsy, S. C.; McElroy, M. B.; Sze, N. D. *Science* **1975**, *187*, 535. (e) Molina, L. T.; Molina, M. J. *J. Phys. Chem.* **1987**, *91*, 433.

(3) Wayne, R. P. *Chemistry of Atmospheres*; Clarendon Press: Oxford, 1991.

(4) (a) Toohey, D. W.; Brune, W. H.; Anderson, J. G. *Int. J. Chem. Kinet.* **1988**, *20*, 131 and references therein. (b) Nicovich, J. M.; Kreutter, K. D.; Wine, P. H. *Int. J. Chem. Kinet.* **1990**, *22*, 399 and references therein.

(5) (a) Prasad, S. S.; Adams, W. M. *J. Photochem.* **1980**, *13*, 243. (b) Prasad, S. S. *Nature*, **1980**, *285*, 152.

(6) Carter, R. O., III.; Andrews, L. J. *J. Phys. Chem.* **1981**, *85*, 2351.

(7) (a) Rathmann, T.; Schindler, R. N. *Chem. Phys. Lett.* **1992**, *190*, 539. (b) Rathmann, T.; Schindler, R. N. *Ber. Bunsen-Ges. Phys. Chem.* **1992**, *96*, 421.

(8) Rauk, A.; Tschuikow-Roux, E.; Chen, Y.; McGrath, M. P.; Radom, L. J. *J. Phys. Chem.* **1993**, *97*, 7947.

(9) (a) McGrath, W. P.; Norrish, R. G. W. *Z. Phys. Chem. (Munich)* **1958**, *15*, 245. (b) McGrath, W. P.; Norrish, R. G. W. *Proc. R. Soc. London, Ser. A* **1960**, *254*, 317.

(10) (a) Baumgärtel, S.; Gericke, K.-H. *Chem. Phys. Lett.* **1994**, *227*, 461. (b) Matsumi, Y.; Nomura, S.; Kawasaki, M.; Imamura, T. *J. Phys. Chem.* **1996**, *100*, 176.

(11) (a) Vanderzanden, J. W.; Birks, J. W. *Chem. Phys. Lett.* **1982**, *88*, 109. (b) Choo, K. Y.; Leu, M. J. *J. Phys. Chem.* **1985**, *89*, 4832.

(12) Farantos, S. C.; Murrell, J. N. *Int. J. Quantum Chem.* **1978**, *14*, 659.

(13) Zhang, J.; Lee, Y. T. *J. Phys. Chem. A* **1997**, *101*, 6485.

(14) Hwang, D.-Y.; Mebel, A. M. *J. Chem. Phys.* **1998**, *109*, 10847.

(15) Lee, T. J.; Allen, W. D.; Schaefer, H. F. *J. Chem. Phys.* **1987**, *87*, 7062.

(16) Adler-Golden, S. M.; Langhoff, S. R.; Bauschlicher, C. W.; Garney, G. D. *J. Chem. Phys*. **1985**, *83*, 255.

(17) Magers, D. H.; Lipscomb, W. N.; Bartlett, R. J.; Stanton, J. F. *J. Chem. Phys*. **1989**, *91*, 1945.

(18) Leininger, M. L.; Schaefer, H. F., III. *J. Chem. Phys*. **1997**, *107*, 9059.

(19) Watts, J. D.; Stanton, J. F.; Bartlett, R. *J. Chem. Phys. Lett*. **1991**, *178*, 471.

(20) Barbre, A.; Secroun, C.; Jouve, P. *J. Mol Spectrosc*. **1974**, *49*, 171.

(21) Murray, C. W.; Handy, N. C.; Amos, R. D. *J. Chem. Phys.* **1993**, *98*, 7145.

(22) Scott, A. P.; Radom, L. *J. Phys. Chem.* **1996**, *100*, 16502.

(23) Rappe, A. K.; Bernstein, E. R. *J. Phys. Chem. A* **2000**, *104*, 6117.

(24) (a) Burke, K.; Perdew, J. P.; Wang, Y. In *Electronic Density Functional Theory: Recent Progress and New Directions*; Dobson, J. F., Vignale, G., Das, M. P., Eds.; Plenum: New York, 1998. (b) Perdew, J. P. In *Electronic Structure of Solids '91*; Ziesche, P., Eschrig, H., Eds.; Akademie Verlag: Berlin, 1991; p 11. (c) Perdew, J. P.; Chevary, J. A.; Vosko, S. H.; Jackson, K. A.; Pederson, M. R.; Singh, D. J.; Fiolhais, C. *Phys. Rev.* **1992**, *B46*, 6671. (d) Perdew, J. P.; Chevary, J. A.; Vosko, S. H.; Jackson, K. A.; Pederson, M. R.; Singh, D. J.; Fiolhais, C. *Phys. Rev.* **1993**, *B48*, 4978. (e) Perdew, J. P.; Burke, K.; Wang, Y. *Phys. Rev.* **1996**, *B54*, 16533.

(25) Frisch, M. J.; Trucks, G. W.; Schlegel, H. B.; Scuseria, G. E.; Robb, M. A.; Cheeseman, J. R.; Zakrzewski, V. G.; Montgomery, J. A., Jr.; Stratmann, R. E.; Burant, J. C.; Dapprich, S.; Millam, J. M.; Daniels, A. D.; Kudin, K. N.; Strain, M. C.; Farkas, O.; Tomasi, J.; Barone, V.; Cossi, M.; Cammi, R.; Mennucci, B.; Pomelli, C.; Adamo, C.; Clifford, S.; Ochterski, J.; Petersson, G. A.; Ayala, P. Y.; Cui, Q.; Morokuma, K.; Malick, D. K.; Rabuck, A. D.; Raghavachari, K.; Foresman, J. B.; Cioslowski, J.; Ortiz, J. V.; Stefanov, B. B.; Liu, G.; Liashenko, A.; Piskorz, P.; Komaromi, I.; Gomperts, R.; Martin, R. L.; Fox, D. J.; Keith, T.; Al-Laham, M. A.; Peng, C. Y.; Nanayakkara, A.; Gonzalez, C.; Challacombe, M.; Gill, P. M. W.; Johnson, B. G.; Chen, W.; Wong, M. W.; Andres, J. L.; Head-Gordon, M.; Replogle, E. S.; Pople, J. A. *Gaussian 98*, revision *A.7*; Gaussian, Inc.: Pittsburgh, PA, 1998.

(26) Gonzalez, C.; Schlegel, H. B. *J. Phys. Chem.* **1990**, *94*, 5523.

(27) Hrusak, J.; Iwata, S. *J. Chem. Phys.* **1997**, *106*, 4877.

(28) Jensen, F. *Introduction to Computational Chemistry*; John Wiley and Sons: New York, 1999; p 189.